atmosphere

MDPI

Article

First Evidences of Methyl Chloride (CH_3Cl) Transport from the Northern Italy Boundary Layer during Summer 2017

Paolo Cristofanelli [1,*], Jgor Arduini [1,2], Francescopiero Calzolari [1], Umberto Giostra [2], Paolo Bonasoni [1] and Michela Maione [1,2]

[1] Institute of Atmospheric Sciences and Climate, National Research Council of Italy, Via Gobetti 101, 40129 Bologna, Italy; jgor.arduini@uniurb.it (J.A.), f.calzolari@isac.cnr.it (F.C.), p.bonasoni@isac.cnr.it (P.B.), michela.maione@uniurb.it (M.M.)

[2] Department of Pure and Applied Sciences, University of Urbino "Carlo Bo", 61029 Urbino, Italy; umberto.giostra@uniurb.it

* Correspondence: p.cristofanelli@isac.cnr.it

Received: 30 January 2020; Accepted: 27 February 2020; Published: 29 February 2020

Abstract: Methyl Chloride (CH_3Cl) is a chlorine-containing trace gas in the atmosphere contributing significantly to stratospheric ozone depletion. While the atmospheric CH_3Cl emissions are predominantly caused by natural sources on the global budget, significant uncertainties still remain for the anthropogenic CH_3Cl emission strengths. In summer 2007 an intensive field campaign within the ACTRIS-2 Project was hosted at the Mt. Cimone World Meteorological Organization/Global Atmosphere Watch global station (CMN, 44,17° N, 10,68° E, 2165 m a.s.l.). High-frequency and high precision in situ measurements of atmospheric CH_3Cl revealed significant high-frequency variability superimposed on the seasonally varying regional background levels. The high-frequency CH_3Cl variability was characterized by an evident cycle over 24 h with maxima during the afternoon which points towards a systematic role of thermal vertical transport of air-masses from the regional boundary layer. The temporal correlation analysis with specific tracers of anthropogenic activity (traffic, industry, petrochemical industry) together with bivariate analysis as a function of local wind regime suggested that, even if the role of natural marine emissions appears as predominant, the northern Italy boundary layer could potentially represent a non-negligible source of CH_3Cl during summer. Since industrial production and use of CH_3Cl have not been regulated under the Montreal Protocol (MP) or its successor amendments, continuous monitoring of CH_3Cl outflow from the Po Basin is important to properly assess its anthropogenic emissions.

Keywords: CH_3Cl; anthropogenic sources; anthropogenic emissions; Italy

1. Introduction

Methyl chloride, CH_3Cl, is a major carrier of reactive chlorine into the stratosphere and the understanding of its natural and anthropogenic sources is important for the further development of global policies on ozone-depleting chemicals [1]. CH_3Cl has become increasingly important as a source of chlorine to the stratosphere, as the abundances of anthropogenic halogenated trace gases have been declining under the Montreal Protocol (MP) regulation [2]. Our current understanding is that CH_3Cl is largely natural in origin: the largest natural sources are tropical vegetation (e.g., [3]), biomass burning (e.g., [4]), oceans (e.g., [5,6]), and salt marshes (e.g., [7]), while the major sinks include oxidation by the hydroxyl radical (OH), uptake by soils, degradation in oceans, and photolysis in the stratosphere. While recent studies have contributed to a better understanding of

emissions from natural sources (e.g., [8–10]), the CH_3Cl global budget still remains unbalanced [2]. Such uncertainties are relevant for policy formulation including CH_3Cl when compared with other anthropogenic ozone-depleting chemicals. Furthermore, emission strengths from anthropogenic sources are still affected by important uncertainties at the global scale (e.g., coal combustion was estimated ranging from of 29 to 295 Gg/year, see [2]). Anthropogenic sources include coal combustion for industrial and incineration activities and indoor biofuel use [2,11] as well as chemical feedstock or solvent releases [12]. Even if the large uncertainty of the source and sink estimations could justify the 20% gap in the global budget of CH_3Cl [13], the recent work by [12] suggested that unaccounted emissions from the chemical industry can help in closing this gap [13]. Interestingly, because the use as chemical feedstock is not supposed to release CH_3Cl to the atmosphere, this has not been taken into account in the national inventory reports (NIRs) submitted to the United Nation Framework Convention for Climate Change (UNFCCC).

On the global scale, extensive regular CH_3Cl measurements are conducted by the Advanced Global Atmospheric Gases Experiment (AGAGE, [14]), and by NOAA-ESRL (National Oceanic and Atmospheric Administration, Earth System Research Laboratory). As reported in the latest Stratospheric Ozone Assessment [13], the 2016 CH_3Cl global mean mole fraction was 553 and 559 ppt (parts per trillion, AGAGE and NOAA measurements, respectively). These values are around 2%–3% higher than the 2012 values reported in the previous Assessment [2], although such changes are thought to be consistent with historical variability. As a consequence of such an increase and of the decrease in regulated anthropogenic chlorinated gases, the fractional contribution to total tropospheric chlorine due to CH_3Cl is currently 16.9% [13].

When focusing on a regional scale, hereinafter referred to as the 20–200 km (meso-beta) scale, modelling studies indicate that the number of measurement sites is still insufficient to constrain the distribution and magnitude of CH_3Cl sources at that specific scales [8,15]. In particular, observations in the outflow of the important source regions should be used to effectively constrain estimates of this source and thus contribute to improving the global CH_3Cl budget.

In this study, for the first time, it is proposed that a highly populated and industrialized area at mid-latitude, such as the Po Basin in northern Italy, may be a non-negligible source area of CH_3Cl. Due to its widespread industrial activities and the high level of household emissions [16], it is of special interest to converge towards a consistent assessment of northern Italy as a CH_3Cl emitter. This assessment would take advantage from the high frequency measurements at the World Meteorological Organization/Global Atmosphere Watch (WMO/GAW) global station of Mt. Cimone (CMN, 2165 m a.s.l.), also part of the global network AGAGE. In summer 2017, the international experimental ACTRIS (Aerosol, Clouds and Trace Gases Research Infrastructure) 2017 campaign, devoted to the investigation of vertical transport of air-masses from northern Italy to the free troposphere, was hosted at the site [17]. Because it overlooks the Po basin, CMN represents a perfect site to investigate the impact of anthropogenic emissions on the regional atmospheric background and on the free troposphere. Here, we discuss the variability of CH_3Cl during June–August 2017 at CMN by analysing the correlations over different time scales (from the 4–5 days typical of the synoptic scale to the hourly scale) with several anthropogenic pollution tracers (e.g., Non-Methane Volatile Compounds (NM-VOCs), carbon monoxide, nitrogen dioxide, sulphur dioxide) and meteorological parameters. A further interesting possibility is related to the availability of carbonyl sulphide (COS) observations at CMN. This atmospheric tracer shares, on the global budget, both natural (mainly wetlands and oceans) and anthropogenic sources [12,18,19].

The aim of this work is to provide a first preliminary understanding about the possible sources of CH_3Cl over northern Italy. The use of several atmospheric trace gases used to trace different anthropogenic sources allowed us to derive first hints about those sectors contributing to the observed variabilities. We primarily focus on interpreting observations at CMN in terms of anthropogenic sources. In particular, we used CH_2Cl_2 as an emission tracer for industrial solvents usage, and HCFC-22 to trace fugitive emissions in hydrofluorocarbons (HFCs) and hydrochlorofluorocarbons (HCFCs) production processes [12]. Indeed, HCFC-22 is supposed to be co-emitted with CH_3Cl and it was used as a robust tracer in a previous CH_3Cl assessment study [2].

Further important hints come from the analysis of 12 anthropogenic NM-VOCs that can trace both combustion and evaporative emissions due to their presence in vehicular emissions or their production in petrochemical processes.

2. Experiments

2.1. Measurement Site

CH_3Cl and other atmospheric tracers are measured since 2002 at Mt. Cimone (2165 m a.s.l.; see Figure 1), which is the highest peak of the northern Apennines ridge and overlooks the Po basin (towards NW–SE) and northern Tuscany (towards S–NW). This particular location, together with the typical meteorological conditions affecting the summer season in this region of the Mediterranean basin (i.e., hot summer with anticyclonic conditions) allows the observation of the upward transport of air-masses from the planetary boundary layer (PBL). Indeed, the vertical transport related to the daytime growth of the mixed layer and the onset of valley and upslope winds during daytime (see e.g., [20]), allow air-masses originating from northern Italy and affected by surface emissions to be caught at this measurement site. Conversely during nighttime, when the measurement site is well above the nocturnal boundary layer, CMN observations can be considered more representative of the background conditions or of aged emissions related both to long-range transport and to residual layers reminiscent of the daytime upward transport of air-masses from the regional boundary layer.

Figure 1. Geographical location of CMN (triangle) in northern Italy. Location of major urban areas (squares) and power/petrochemical plants (polygons) are also reported.

2.2. Measurement of CH_3Cl and Other Atmospheric Trace Gases

At CMN, several programs for the continuous monitoring of trace gases are carried out on a systematic basis. CH_3Cl, CH_2Cl_2, HCFC-22, COS and 12 non-Methane Volatile Organic Compounds are measured by an Agilent 6850–5975 GC–MS (Agilent, Santa Clara, CA, USA) equipped with the UNITY2-Air Server2 auto-sampling/pre-concentration device (Markes International, Llantrisant, UK). The ambient air sample is analysed every two hours and two working standard runs bracket every air sample run, in order to detect and correct for short-term instrumental drift. The working standards for CH_3Cl, CH_2Cl_2 and HCFC-22 are regularly calibrated (weekly) against a tertiary standard prepared with the same procedure at the baseline station of Mace Head (Ireland). They are calibrated on the SIO-05, SIO-07, SIO-014 scales developed and maintained at Scripps Institute of Oceanography (San Diego CA, USA) where primary gravimetric standards are prepared to be used in the AGAGE stations. NM-VOC working standards are referenced against a reference standard by NPL (National Physical Laboratory, Teddington, UK). The NPL gas mixture contains 30 ozone precursor hydrocarbon compounds listed in Annex X of the European Directive 2008/50/EC on

Ambient Air Quality and Cleaner Air for Europe, at nominal concentrations of 4 nmol/mol, with actual certified concentration ranging from 3.59 to 4.28 ± 0.07 nmol/mol; absolute concentrations are propagated to a lower concentration standard in air that is used to calibrate the working standard. For CH_3Cl and NM-VOCs annual mean relative standard deviations (RSD) are evaluated from the repeated working standard measurements. Measurement repeatability (evaluated from repeated working standards measurements) for CH_3Cl, CH_2Cl_2, HCFC-22 and COS ranged from 0.3% to 5%. Limits of detection (LODs) are in the ranges of 0.06–0.20 ppt. For the considered NM-VOCs these values ranged from 0.7% to 2.9% and around 1.0 ppt, respectively. More details about CH_3Cl and NM-VOC measurements can be found in [21,22].

During summer 2017, CO was measured by non-dispersive infra-red (NDIR) technique. The system is based on a Tei48C-TL analyser (Thermo Fischer Scientific, Waltham, MA, USA) which uses gas filter correlation technology for determining CO ambient concentration. With the aim of minimizing possible influence of water vapor in the NDIR detection, the ambient air passes through a drying system (Nafion© dryer) and is then injected in the measurement cell (more details can be found in [21]). A correction based on the results of a span check is performed once a day, while every 3 months a multipoint calibration is carried out by using a set of 6 NOAA standards. In this way, the measurements are referred to the WMO CO_*X2014A* calibration scale. NO_2 observations were continuously carried out by using a chemioluminescence analyser (Tei42i-TL, Thermo Fischer Scientific, Waltham, MA, USA) equipped with a photolytic converter (Blue Light Converter by Air Quality Design). Every 48 h, zero and span checks are carried out for NO by using an external zero air source (Thermo 1160 dry air generator equipped with Purafill© and active charcoal scrubbers, Thermo Fischer Scientific, Waltham, MA, USA) and dilution of certified NO mixture in N_2 (5 ppm ± 3.5% by NPL). To determine the efficiency of the NO_2 photolytic converter, gas phase titration (GPT) is used to titrate about 80% of the NO obtained by dilution. SO_2 observations were based on a 43iTLE (Thermo Fischer Scientific, Waltham, MA, USA), which is based on the UV-fluorescence technology. Daily execution of zero/span checks were carried out by an internal span source (permeation tube with emission rate of 44 ng/min ± 10%) and external zero source (activated charcoal filled cartridge). A dilution system (Environics 4000) was used to perform multi-point calibration (range: 0.5–10 ppb) from a certified standard of 100 ppb SO_2 in N_2 (s/n: 12048642) provided by NPL.

3. Results

As shown by [23], the seasonal variability of CH_3Cl in the northern hemisphere is characterized by a late summer minimum (August–September), which is attributed primarily to the seasonal change in OH [24]. During summer (June–August) 2017, the CH_3Cl mean value was 556.9 ± 2.3 ppt (± 95% confidence level), compared with the concomitant mean value of 540 ppt (R: 0.62, $p < 0.01$) derived by AGAGE observations at the Jungfraujoch station (3580 m a.s.l., Swiss Alps). The deviation between CMN and Jungfraujoch observations is reduced when only nighttime data are considered for CMN (550.6 ± 2.1 ppt): the higher values observed at CMN can be attributed to the stricter proximity to emission sources.

Figure 2 reports the time series of CH_3Cl (red) for the ACTRIS experiment at CMN, together with CO (black), air-temperature (grey) and atmospheric pressure (blue). For CH_3Cl, variabilities occurring at different time scales are evident: a 24 hour-scale variability is superimposing a multiday component. To filter out this variability at longer time scales, we applied a Loess interpolation [25] to the original time series (thick lines). The smoothed time series showed a certain degree of co-variability between CH_3Cl and CO, a well-known tracer of combustion processes, over time scale of a few days which mimic the behaviour of meteorological parameters. To compare the relative importance of the day-to-day against the diel variability for CH_3Cl, we calculated the standard deviation of the hourly and smoothed datasets [26,27]: sd_{hourly} (28.6 ppt) and $sd_{smoothed}$ (23.2 ppt), respectively. Since with the smoothed dataset the diel component of CH_3Cl variability are filtered out, the comparison between the dataset standard deviation allows us to discriminate the hourly variability from other sources of variability. We obtained a ratio $sd_{hourly}/sd_{smoothed}$ equal to 0.81,

indicating that the diel variability represented about one fifth of the total CH_3Cl variability observed at CMN during summer 2017.

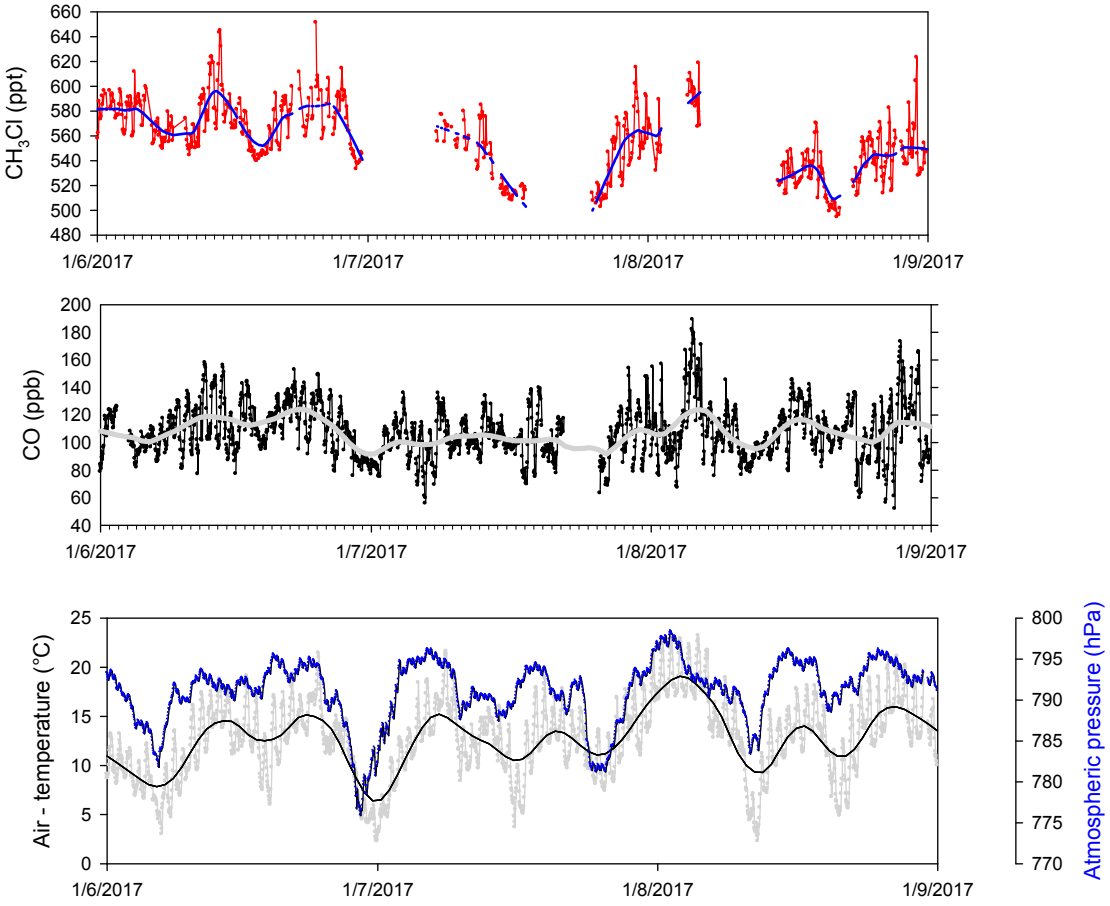

Figure 2. Time series of CH_3Cl, CO, air-temperature and pressure observed at CMN during summer 2017. The tick lines represent the Loess smoothing.

To provide first hints about the source of the diel variability, we compared (Figure 3) the 24 h variability of CH_3Cl with tracers of combustion processes (i.e., CO, NO_2 and SO_2). In particular, CO is a valuable tracer of direct emissions from fossil fuels and biomass combustion, SO_2 is primarily emitted by fossil fuel combustion in industrial processes and energy production, while anthropogenic emissions of NO_2 encompassed high temperature combustion of fossil fuels in electricity generation and petroleum based motors and by lower temperature combustion of biomass in wildfires, deforestation and domestic burning [28]. With the purpose of better characterising the 24 h evolution of CH_3Cl, the variability of O_3/NO_x was also considered (Figure 4); according to [29,30] this ratio can be considered as a proxy to qualitatively evaluate the proximity to major emission sources and photochemical processing. The O_3/NO_x variability already provided useful information to disentangle the role of "fresh" versus "aged" anthropogenic pollution in affecting summer atmospheric composition variability at CMN [20]. As shown in Figures 3–4, the afternoon increase in CH_3Cl values was concomitant with an increase in combustion tracers (SO_2 and CO) and a decrease in the O_3/NO_x ratio, which supports the advection of PBL air-masses towards the measurement site due to the thermal transport.

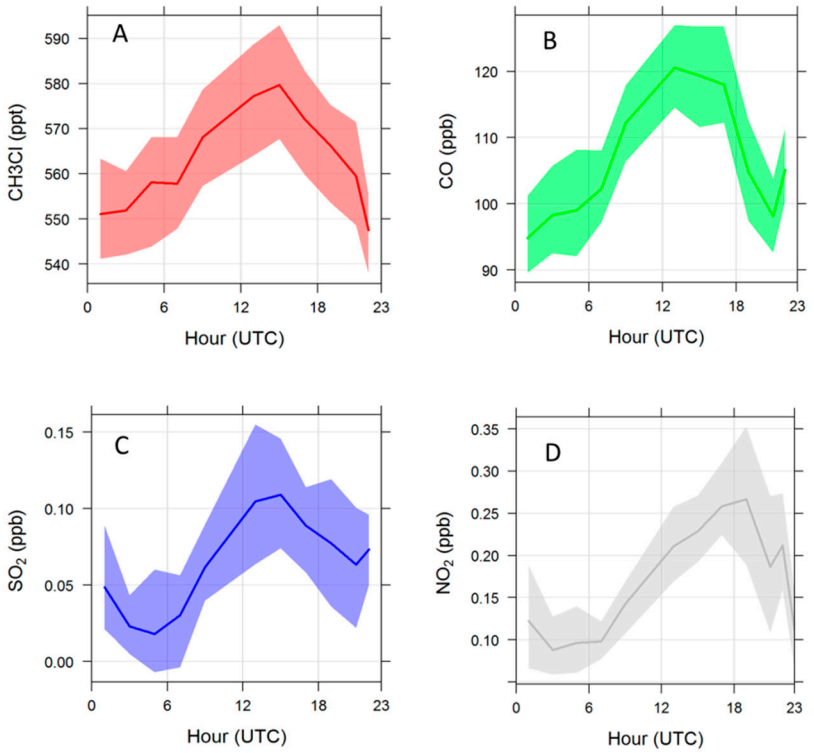

Figure 3. Averaged diel variation of CH_3Cl (**A**), CO (**B**), SO_2 (**C**) and NO_2 (**D**) during summer 2017. The shaded area denotes the 95% confidence level.

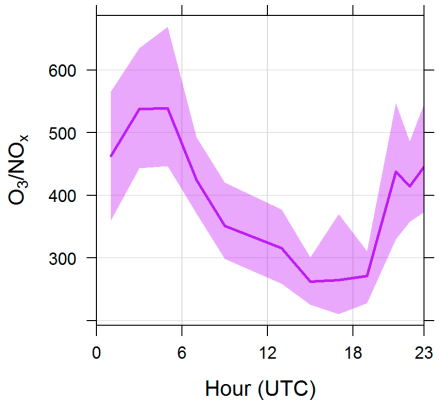

Figure 4. Averaged diel variation of O_3/ NO_x during summer 2017. The shaded area denotes the 95% confidence level.

3.1. Correlation Analysis of CH_3Cl with Other Tracers: Smoothed Datasets

To identify possible contributions driving the variability of CH_3Cl over a low frequency scale, typical of the synoptic time scales, we analysed the multiple correlations between the smoothed datasets of CH_3Cl and other anthropogenic trace gases including COS, CH_2Cl_2, HCFC-22, CO, SO_2 and those NM-VOCs (ethyne, propane, benzene) which, according to [22], have a typical summer atmospheric lifetime exceeding 7 days and can thus be used to trace long-range transport (see Figure 5). These trace gases have been selected based on their relatively long atmospheric lifetimes, with the aim of minimising possible interference from local sources characterised by the presence of highly reactive NM-VOCs. NO_2 was not considered to avoid introducing inconsistencies related to its non-linear participation in the photochemical reactions. According to [12], COS was included as tracer for

biomass/biofuel/coal combustions (included industrial aluminium production), CH_2Cl_2 is suggested to be an emission tracer for industrial solvent usage, while HCFC-22 is used to trace possible co-located industrial emissions. Indeed, HCFC-22 is used as feedstock for Poly-Tetra-Fluoro-Ethylene (PTFE), for which production plants are located in the Po Basin. However, it should be taken into account that at the global scale COS is also affected by significant natural emission [19]. Besides analysing the cross linear correlation between the considered trace gases, we also carried out a hierarchical cluster analysis with the purpose of grouping together the different atmospheric trace gases which are related to each other. Indeed, the application of the cluster analysis would provide a rough identification of those compounds sharing the same source processes [31]. To this aim, we used the Pearson linear correlation as a metric of the distance among the single elements (i.e., the time series of each single trace gas). With the aim of assessing the impact of different agglomeration methods in the clustering results, three different agglomeration methods have been used: "single linkage", "complete linkage", and "Ward". In the following, the clustering results for the "complete" linkage are shown. Similarities and differences between the clustering runs with different agglomeration methods are discussed in Section 4.

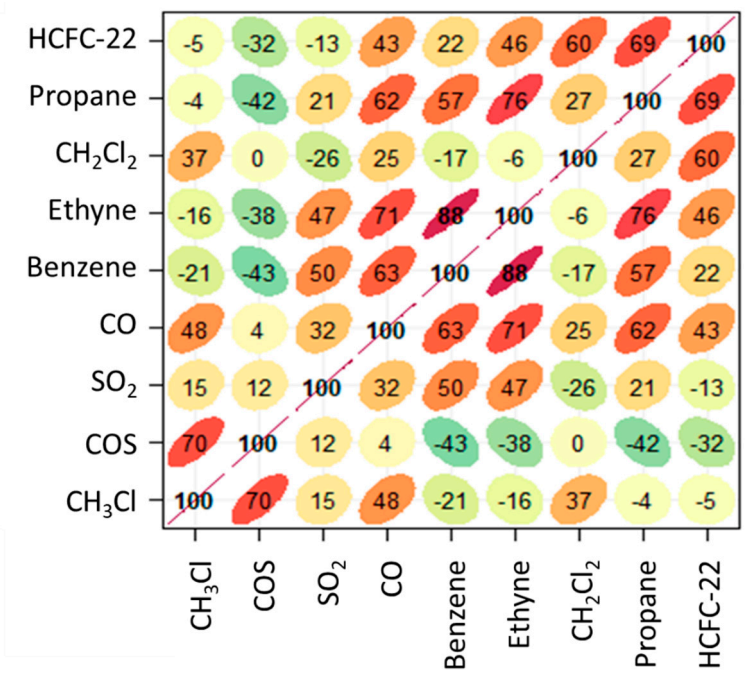

Figure 5. Multiple correlation analysis of the smoothed dataset for summer 2017. The shape of ellipses provides a visual representation of the scatter plot for each couple of variables, the numbers and the colour code give representation of the R value (green: negative slope of correlation, red: positive slope of correlation).

The correlation profile for the smoothed datasets showed that CH_3Cl had the highest positive correlation ($R = 0.70$, $p < 0.01$) with COS. A relatively high correlation was also found with CO ($R = 0.48$, $p < 0.01$). This would support a possible role of emissions related to or co-located with combustion processes. Taking into account the relatively long tropospheric lifetime of CO (~3 months, see [28]) it can be argued that this would trace aged combustion emissions. A relatively low positive correlation ($R = 0.37$, $p < 0.01$) with CH_2Cl_2 would suggest a secondary role of evaporative or fugitive emissions related to industrial production processes. Further hints for attributing the variability of CH_3Cl on a synoptic scale can be obtained by the hierarchical cluster analysis reported by the dendrogram in Figure 6, which provides additional information by visualising how groups of variables are related to one another.

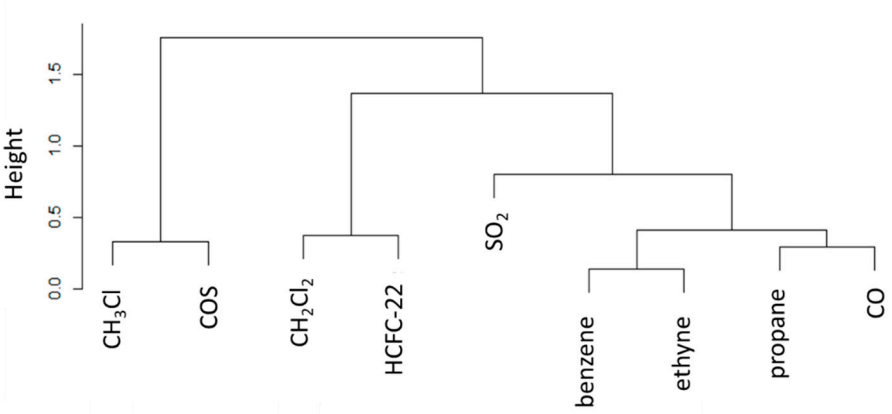

Figure 6. Dendrogram of cluster analysis of atmospheric trace gases for the smoothed dataset. Note that the y-axis denotes the cluster distance (indicated as "height").

From the cluster aggregation, it is clear that CH_3Cl and COS share a high degree of similarity in their variability and behave differently than the other trace gases. Indeed, other compounds sharing variability are ethyne-benzene and propane-CO (tracing emissions from vehicular emission exhausts). These two clusters (not related to CH_3Cl) are also grouped with SO_2, further supporting the role of combustion emissions (fossil fuels). CH_2Cl_2 and HCFC-22, combined together, clearly trace emissions from fugitive sources related to PTFE production process (HCFC-22) and industrial solvents usage (CH_2Cl_2). According to [7], anthropogenic sources of COS appear to be mostly concentrated in Asia and related to Rayon production, but important emissions are still associated to aluminium production, coal use and biomass burning (biofuels, open burning, and agriculture fires). [19] suggested that, even if anthropogenic (+400 ± 140 Gg S yr^{-1}) and biomass burning (+116 ± 52 Gg S yr^{-1}) emissions are dominant on the global scale, natural emissions (ocean: +265 ± 210 Gg S yr^{-1}; wetlands: −150 to + 290) are significant. In our case, the strong similarity of CH_3Cl with COS and the high cluster distance with unambiguous anthropogenic tracers (i.e., CH_2Cl_2, and HCFC-22) and CO, suggest that the synoptic-scale variability of CH_3Cl can be primarily related to natural emissions, most likely related to oceans.

3.2. Correlation Analysis of CH_3Cl with Other Tracers: Residual Analysis

To obtain information about possible local anthropogenic sources of CH_3Cl at CMN, we analysed the time series of trace gas residuals, i.e., the difference between the punctual measurements with the smoothed dataset obtained by the application of the Loess regression. This analysis is intended to provide complementary information with respect to Section 3.1, where the variability on longer time scales is considered. For this purpose, two different temporal windows of data have been considered: residuals for daytime (12–18 UTC) and for night-time (0–4 UTC). To specifically diagnose fresh emissions occurring from the local to the regional scale, selected reactive compounds have been introduced in the analysed dataset. Among the NM-VOCs measured at CMN, we have considered those which are characterised by relatively low summer reactivity with respect to OH, i.e., toluene, pentanes, butanes, propane, benzene and ethyne (see [22]). For pentanes and butanes, only one isomer has been considered (i-butane and i-pentane, namely) because of their very high cross correlation. The correlation and the cluster analysis were carried out for the original time resolution, with the purpose of retaining the highest degree of information from the datasets. This choice would disentangle the different conditions characterised by daytime upward thermal transport (i.e., direct influence of air-masses from the regional PBL, as suggested in Section 3.1) and more aged (background) air-masses during nighttime [20]. With respect to the previous analysis a larger number of trace gases has been considered.

For the daytime dataset of residuals (Figure 7), CH_3Cl mostly correlates with benzene ($R = 0.53$, $p < 0.01$), ethyne (0.48, $p < 0.01$), CO ($R = 0.50$, $p < 0.01$) and n-octane (0.47 $p < 0.01$). In general, the highest (positive) correlation was found for CO and the anthropogenic NM-VOCs, thus supporting

a role of anthropogenic emission (possibly co-located with combustion emission) in affecting the variability of CH_3Cl during daytime at CMN. The degree of correlation appeared to be slightly higher with NM-VOCs characterized by higher lifetime with respect to OH mixing ratios (i.e., ethyne, benzene) and lower for the more reactive toluene ($R = 0.40$, $p < 0.01$). In contrast to the smoothed dataset, a weak negative correlation was found between CH_3Cl and COS for the residuals. This can be explained by considering the inverse diel variability which characterizes COS during summer 2017 at CMN (i.e., high values during nighttime versus lower values during daytime). On the other hand, this can further stress the relative decoupling of CH_3Cl and COS variability during daytime at CMN (this latter being also influenced by photosynthetic activity of vegetation [19]).

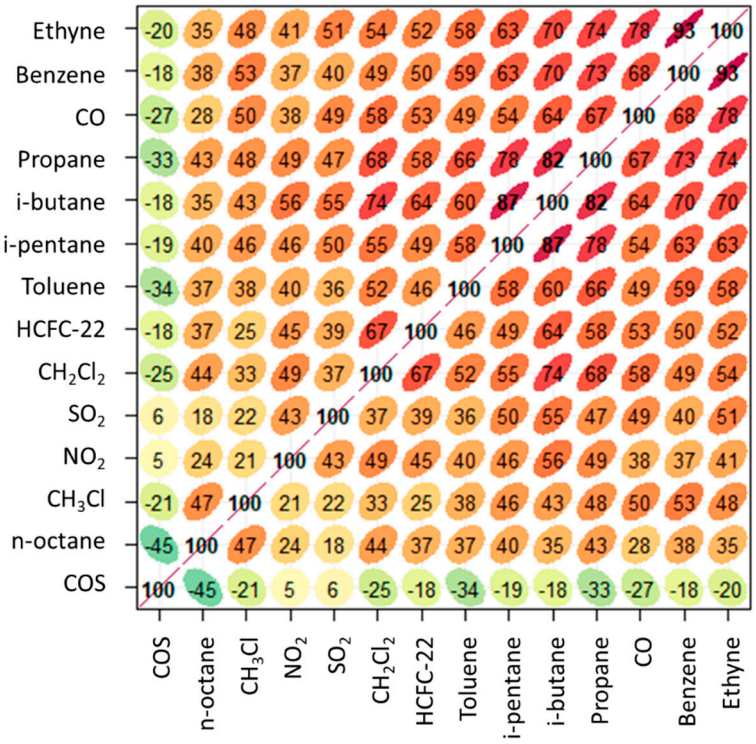

Figure 7. Multiple correlation analysis of the daytime dataset for summer 2017. The shape of ellipses provides a visual representation of the scatter plot for each couple of variables, the numbers and the colour code give representation of the R value (green: negative slope of correlation, red: positive slope of correlation).

According to the cluster analysis (Figure 8), the strongest similarity is found between CH_3Cl and those anthropogenic NM-VOCs that were identified by [22] as tracers of fuel evaporation (i.e., pentane, octane and butane) and industrial solvent (i.e., toluene). In particular, the lowest distance was found for toluene and octane. Other clusters (but with lower similarity to CH_3Cl) appeared to be related to vehicular fuel combustion (i.e., CO, benzene, ethyne) and fugitive industrial emissions (CH_2Cl_2 and HCFC-22). This clustering analysis confirms the "independent" behaviour of COS during summer daytime at CMN with respect to other anthropogenic tracers.

For the nighttime dataset of residuals (Figure 9), CH_3Cl showed a high correlation with CO ($R = 0.57$, $p < 0.01$), benzene, propane, ethyne (R from 0.50 to 0.45, $p < 0.01$), which are the least reactive compounds, suggesting that they can describe contributions of air masses that underwent more aged transport of automobile exhausts, fuel evaporation and generation of Liquified Petroleum Gas-LPG (ethyne, benzene and propane). A not negligible positive correlation was found also between CH_3Cl and butane ($R = 0.44$, $p < 0.01$), a more reactive trace gas (estimated lifetime with respect to OH lower than 1 day in summer, [22]) associated to fuel evaporation.

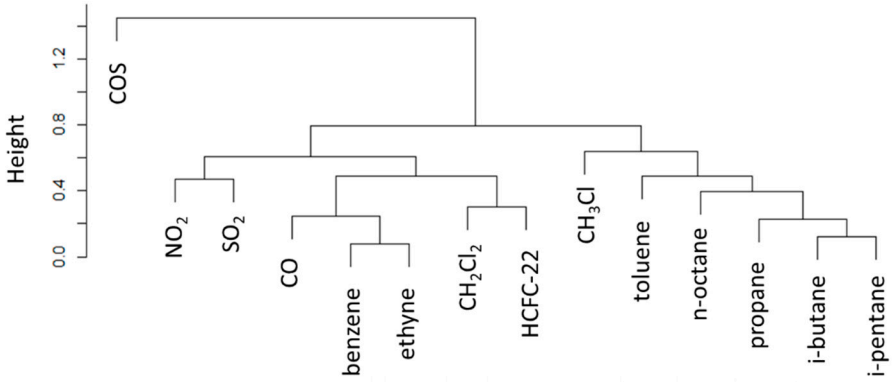

Figure 8. Dendrogram of cluster analysis of atmospheric trace gases for the residuals of the daytime (12:00–18:00 UTC) dataset. Note that the y-axis denotes the cluster distance (indicated as "height").

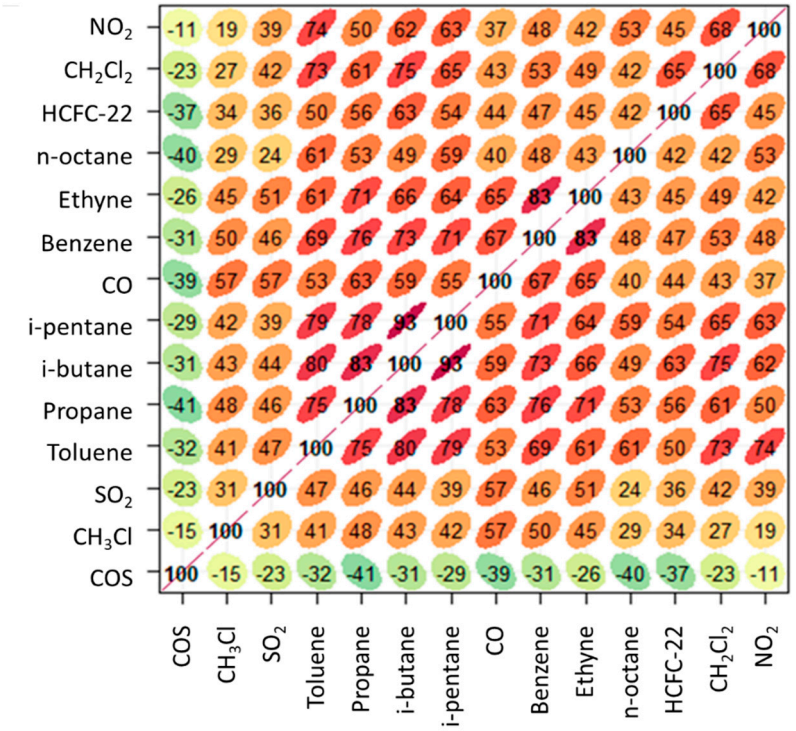

Figure 9. Multiple correlation analysis of the nighttime dataset for summer 2017. The shape of ellipses provides a visual representation of the scatter plot for each couple of variables, the numbers and the colour code give representation of the R value (green: negative slope of correlation, red: positive slope of correlation).

Looking at the cluster analysis reported in Figure 10, similarities between CH_3Cl and the other trace gases are less pronounced. This is probably related to the fact that during nighttime CMN is well decoupled from the regional PBL and the higher degree of dynamic mixing of air-masses reaching the measurement site during nighttime reduces the typical emission fingerprints. However, in general, CH_3Cl appeared to be decorrelated also from COS (due to the negative linear correlation between them). The mixing occurring in the free troposphere probably has the larger influence on nighttime concentrations.

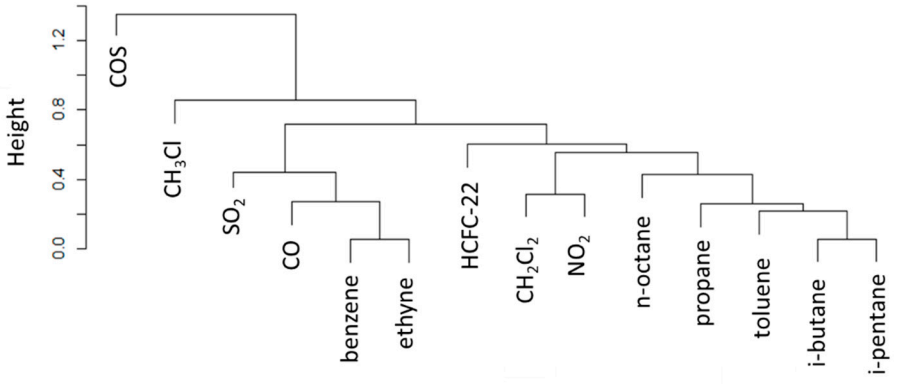

Figure 10. Dendrogram of cluster analysis of atmospheric trace gases for the residuals of the nighttime (00:00–04:00 UTC) dataset. Note that the y-axis denotes the cluster distance (indicated as "height").

3.3. Analysis of CH_3Cl with Local Wind Regime

In an attempt at providing a first spatial identification of regional emissions affecting hourly CH_3Cl enhancements at CMN, we analysed the positive residuals of CH_3Cl and residuals of selected tracers as a function of wind speed and directions during daytime. The choice of restricting our attention only to the daytime time window for this analysis is related to the following reasons. Firstly, during daytime, the thermal transport is active, making observations at CMN more representative of the PBL air masses. Secondly, it is for daytime that we obtained the more robust relationship between CH_3Cl and other trace gases from the cluster analysis.

To this aim, we calculated bivariate polar plots (Figure 11) of mixing ratios [32] for CO (combustion tracer), benzene (as traffic exhaust tracer) and toluene and n-octane (tracers of evaporative emissions): all these trace gases showed a high degree of temporal correlation (like in the case of CO and benzene) or similarity (like in the case of toluene and n-octane) with CH_3Cl, as deduced by the multiple correlation analysis and the clustering. For the sake of completeness, the equivalent nighttime analysis is presented in the supplementary material (SM). Moreover, while CO and benzene are expected to be influenced also by long-range emissions, toluene is expected to be more representative of local/regional emissions due to its shorter atmospheric lifetime. The bivariate analysis has been performed using the "Openair" package [33] included in the "R" Language and Environment for Statistical Computing. Wind speed, wind direction and mixing ratio data are partitioned into wind speed-direction bins and the mean mixing ratio calculated for each bin. The wind components, u and v, are calculated by using the equation:

$$u = \bar{u} \sin(2\pi/\theta),\ v = \bar{u} \cos(2\pi/\theta) \quad (1)$$

where $\bar{u}$ is the mean hourly wind speed and θ is the mean wind direction in degrees, with 90 degrees indicating wind coming from the East. The field of mixing ratio (mr) as a function of ($\bar{u}$, θ) is obtained by using a Generalized Additive Model (GAM), e.g., [34,35] which is useful to model the non-linear relationship between the variables. GAMs can be expressed as follows:

$$\sqrt{\boldsymbol{mr_i}} = \boldsymbol{\beta_o} + \sum_{\boldsymbol{j=1}}^{\boldsymbol{n}} \boldsymbol{s_j}\,(\boldsymbol{x_{ij}}) + \boldsymbol{e_i} \quad (2)$$

where mr_i is the i^{th} pollutant mixing ratio, β_0 is the overall mean of the response, $s_j(x_{ij})$ is the smooth function of i^{th} value of covariate j, n is the total number of covariates, and e_i is the i^{th} residual. More details can be found on [33].

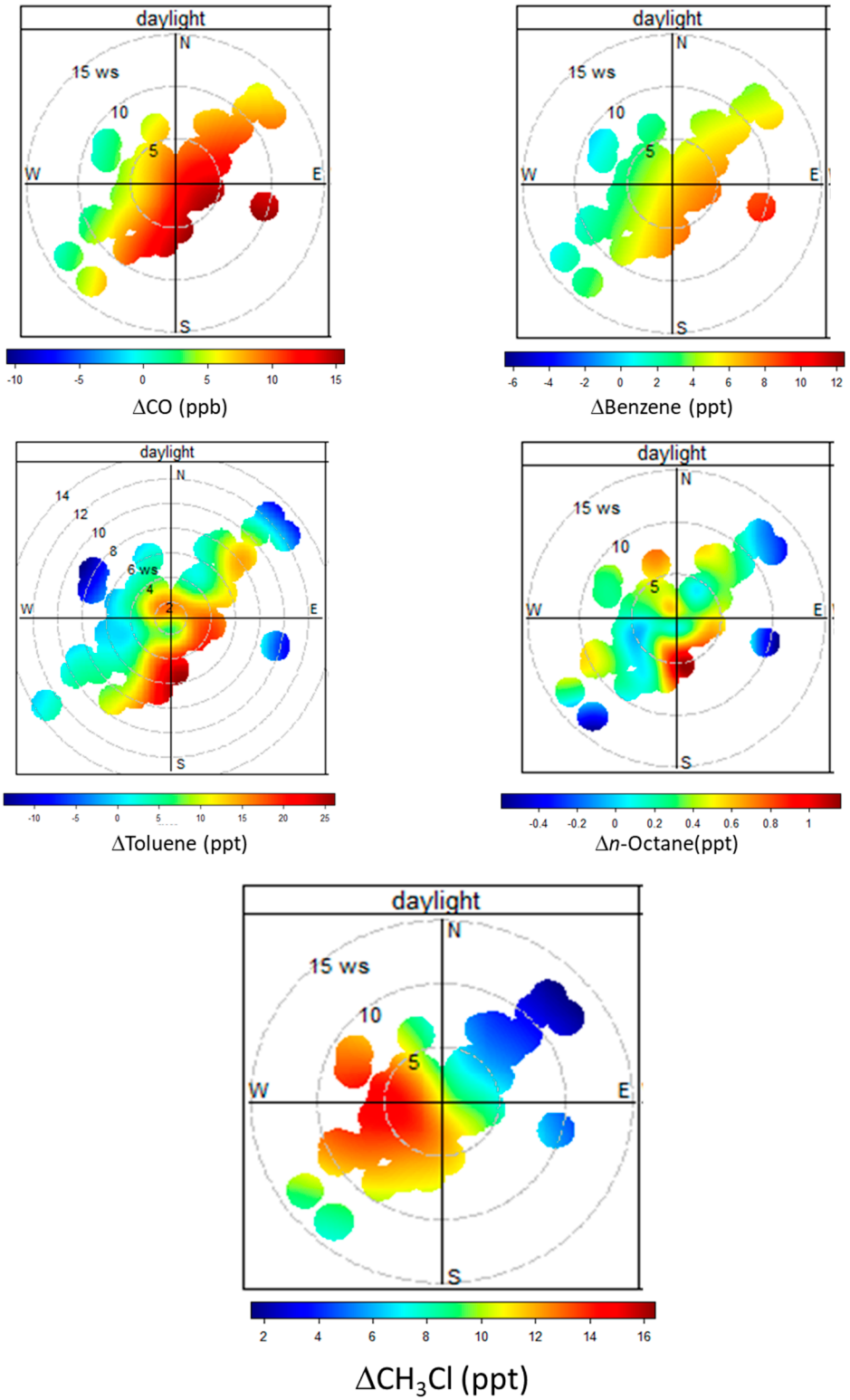

Figure 11. Bivariate analysis of the mean average residuals of CH_3Cl, CO, benzene, toluene, and n-octane for CH_3Cl enhancement events (i.e., positive residuals) during summer 2017 (daytime). Please note that for CH_3Cl only positive enhancements are shown.

Noteworthy, independently of wind speed or direction, CH_3Cl residuals showed only positive values: this would indicate the existence of emissions occurring at regional scale over northern Italy. The largest CH_3Cl enhancements occurred in air masses coming from S to NW and wind speeds of 1 to 10 m/s.

In particular, the high CH_3Cl values associated with wind from S–NW are coherent with the presence of important power production plants (La Spezia and Livorno) and a petrochemical industry (Livorno area), which are located along the western coastlines of northern Italy (see Figure 1) in a range of 60–80 km from CMN and the northern Apennines.

The bivariate analysis of other atmospheric tracers can provide further hints towards the attribution of the CH_3Cl enhancements. In good agreement with the clustering analysis, toluene and n-octane showed large enhancements from the southern sector, for which CH_3Cl is also largely enhanced. Since these NM-VOC are well representative of evaporative sources, this would support an impact from the region South to CMN, where petrochemical plants are located (Figure 1). For CO and benzene, a somewhat different bivariate distribution was observed with respect to toluene and n-octane: during daytime the highest values were associated with air-masses from NE to SW and thus spanning a range of spatial origin encompassing the Po basin, the Florence urban basin as well as the region for which toluene and n-octane enhancements are evident (Figure 1). The high CH_3Cl enhancements along the wind sectors W–NW, would suggest a role of marine emissions from the Thyrrenian Sea which might affect daytime CH_3Cl variability at CMN. Even if a previous summer field campaign assessed the impact of marine emissions to CMN as marginal [36], this possibility can be supported in light of the small enhancements of the most reactive NM-VOCs observed for this sector (e.g., see toluene). For the nighttime selections (see Figure S1), the bivariate analysis provided less consistent results than for the daytime selection. This is in agreement with the dissimilarity observed during nighttime with cluster analysis and can support the possibility of contributions related to large-scale ocean emissions when the measurement site is more exposed to large-scale circulation.

4. Conclusions

We analysed a summer dataset of high frequency CH_3Cl observations at the high mountain station Mt. Cimone (northern Italy). The execution of an intensive field experiment (ACTRIS-2 Mt Cimone and Po Valley Field Campaign 2017) allowed us to perform a first detailed investigation of CH_3Cl variability over the synoptic and 24 h scales. At the synoptic scale, the highest correlations were found with COS ($R = 0.70$), CO ($R = 0.48$) and CH_2Cl_2 ($R = 0.37$). A cluster analysis clearly indicated a similarity between CH_3Cl variability and COS suggesting a dominant role of natural emissions from oceans with respect to anthropogenic sources, which nevertheless contributed to the synoptic scale variability of CH_3Cl at CMN, as deduced by the co-variability with CO and CH_2Cl_2. A sensitivity study was carried out to assess the impact of using different agglomeration methods in the clustering: "single linkage", "multiple linkage", and "Ward". The similarity between CH_3Cl and COS was robust for all the agglomeration methods used.

Similarly to other atmospheric tracers emitted in the northern Italy PBL, CH_3Cl showed a diel cycle with a maximum during late afternoon as results of the occurrence of upward transport of PBL air masses by thermal wind circulation and daytime PBL height growth. The analysis of CH_3Cl multiple correlation revealed co-variability with CO, benzene, ethyne and propane, suggesting the possibility of co-location of CH_3Cl sources with anthropogenic combustions (like vehicular traffic). In particular, a specific role of emissions related to evaporative sources of fuel (i.e., pentane, octane and butane) and industrial solvents (i.e., toluene) was supported by the cluster analysis. This would support a role of petro-chemical or industrial processes. In this case, some differences exist when the various agglomeration methods are considered. The similarity with evaporative-released NM-VOCs (toluene, butane, octane, propane, pentane) is confirmed when the "Ward" agglomeration method is used (here not shown), while in the case of the "single linkage" method, the similarity is higher with SO_2 and NO_2, thus supporting a role of fossil fuel/coal emissions in determining CH_3Cl variability.

Even if far from being conclusive, the bivariate analysis of CH_3Cl as a function of wind direction and speed, suggests the possible existence of anthropogenic sources in the western region of northern Italy, where plants for power production and petrochemical industries are located. The high CH_3Cl enhancements along the wind sectors W-NW would suggest a possible role of the near Tyrrhenian Sea in affecting the daytime CH_3Cl variability at CMN. However, it must be considered that this wind

sector is much less important (in term of frequency) than the SW–S for which we obtained more robust evidence of co-located emission of anthropogenic NM-VOCs. These results would indicate that, during the summer, the northern Italy PBL would represent a source of CH_3Cl for the lower free troposphere of the Mediterranean basin/South Europe thanks to thermal transport along the mixed layer and up-slope/up-valley winds across the Apennine ridge: once transported at the altitude of CMN, material from PBL can be diffused over large distance. Even if a comparative analysis of hour-to-hour vs. day-to-day variability (mostly affected by natural CH_3Cl emissions, as deduced by the high similarity with COS variability) indicated that the former only contributed to 1/5 of the overall CH_3Cl variability, the possible role of emissions from the regional PBL cannot be neglected. Further work, by exploiting the long-term dataset of observations available at CMN, will be carried out to systematically assess the impact of this process for the whole year and to better constraint the identification of the anthropic CH_3Cl sources and the variability of their strength with time. Since industrial production and use of CH_3Cl have not been regulated under the Montreal Protocol (MP) or its successor amendments, continuous monitoring of CH_3Cl outflow from the Po basin is important to properly evaluate its anthropogenic emissions.

Supplementary Materials: The following are available online at www.mdpi.com/2073-4433/11/3/238/s1, Figure S1: Bivariate analysis of mean average residuals of CH_3Cl, CO, benzene, toluene, and n-octane for CH_3Cl enhancement events (i.e., positive residuals) during summer 2017 (nighttime).

Author Contributions: Conceptualization, P.C. and M.M.; methodology, P.C.; U.G.; software, P.C.; formal analysis, P.C.; investigation, P.C.; U.G.; M.M.; resources, P.B.; data curation, F.C.; J.A.; writing—original draft preparation, P.C, M.M..; writing—review and editing, J.A.; U.G..; funding acquisition, P.B. All authors have read and agreed to the published version of the manuscript.

Funding: CO: NO_2: SO_2 and NM-VOC observations during the ACTRIS-2007 summer field campaign were partially supported by the Project of Interest NEXTDATA (supported by MIUR throughout CNR-DTA) and ACTRIS-2 H2020. The publication costs were supported by the CNR-DTA throughout the "Accordo Interistituti ICOS".

Acknowledgments: CNR strongly acknowledges the logistic support and accessibility provided by the Italian Air Force (CAMM) at the Mt. Cimone observatory. We acknowledge the AGAGE Science Team and SIO (Scripps Institution of Oceanography) for providing the calibration standards used at CMN as well as Jungfraujoch CH_3Cl data for summer 2017 (especially M.K. Vollmer, S. Reimann, P.B. Krummel and Ray Wang). The "OpenAir" analysis package for R was obtained from http://www.openair-project.org.

Conflicts of Interest: The authors declare no conflict of interest.

References

1. Clerbaux, C.; Cunnold, D.M.; Anderson, J.; Engel, A.; Fraser, P.J.; Mahieu, E.; Manning, A.; Miller, J.; Montzka, S.A.; Nassar, R.; et al. Long-lived compounds—Chapter 1. In *Scientific Assessment of Ozone Depletion: 2006*; Global Ozone Research and Monitoring Project—Report No. 50; World Meteorological Organization: Geneva, Switzerland, 2007.
2. Carpenter, L.J.; Reimann, S.; Burkholder, J.B.; Clerbaux, C.; Hall, B.D.; Hossaini, R.; Blake, D.R. Update on Ozone-Depleting Substances (ODSs) and Other Gases of Interest to the Montreal Protocol. In *Scientific Assessment of Ozone Depletion: 2014*; Global Ozone Research and Monitoring Project—Report No. 55; World Meteorological Organization: Geneva, Switzerland, 2015.
3. Yokouchi, Y.; Ikeda, M.; Inuzuka, Y.; Yukawa, T. Strong emission of methyl chloride from tropical plants. *Nature* **2002**, *416*, 163–165, doi:10.1038/416163a.
4. Lobert, J.M.; Keene, W.C.; Logan, J.A.; Yevich, R. Global chlorine emissions from biomass burning: Reactive Chlorine Emissions Inventory. *J. Geophys. Res.* **1999**, *104*, 8373–8389, doi:10.1029/1998JD100077.
5. Moore, R.M.; Groszko, W.; Niven, S.J. Ocean-atmosphere exchange of methyl chloride: Results from NW Atlantic and Pacific Ocean studies. *J. Geophys. Res.* **1996**, *101*, 28529–28538, doi:10.1029/96JC02915.
6. Hu, L.; Yvon-Lewis, S.A.; Butler, J.H.; Lobert, J.M.; King, D.B. An improved oceanic budget for methyl chloride. *J. Geophys. Res. Ocean.* **2013**, *118*, 715–725, doi:10.1029/2012JC008196.
7. Rhew, R.C.; Miller, B.R.; Weiss, R.F. Natural methyl bromide and methyl chloride emissions from coastal salt marshes. *Nature* **2000**, *403*, 292–295, doi:10.1038/35002043.

8. Xiao, X.; Prinn, R.G.; Fraser, P.J.; Simmonds, P.G.; Weiss, R.F.; O'Doherty, S.; Miller, B.R.; Salameh, P.K.; Harth, C.M.; Krummel, P.B.; et al. Optimal estimation of the surface fluxes of methyl chloride using a 3-D global chemical transport model. *Atmos. Chem. Phys*. **2010**, *10*, 5515–5533, doi:10.5194/acp-10-5515-2010.
9. Saito, T.; Yokouchi, Y.; Philip, E.; Okuda, T. Bidirectional exchange of methyl alides between tropical plants and the atmosphere. *Geophys. Res. Lett.* **2013**, *40*, 5300–5304.
10. Saito, T.; Yokouchi, Y.; Kosugi, Y.; Tani, M.; Philip, E.; and Okuda, T. Methyl chloride and isoprene emissions from tropical rain forest in Southeast Asia. *Geophys. Res. Lett.* **2008**, *35*, L19812, doi:10.1029/2008GL035241.
11. McCulloch, A.M.; Aucott, L.; Benkovitz, C.M.; Graedel, T.E.; Kleiman, G.P.; Midgley, M.; Li, Y.-F. Global emissions of hydrogen chloride and chloromethane from coal combustion, incineration and industrial activities: Reactive Chlorine Emissions Inventory. *J. Geophys. Res.* **1999**, *104*, 8391–8404, doi:10.1029/1999JD900025.
12. Li, S.; Park, M.-K.; Jo, C.O.; Park, S. Emission estimates of methyl chloride from industrial sources in China based on high frequency atmospheric observations. *J. Atmos. Chem*. **2017**, *74*, 227–243.
13. Engel, A.; Rigby, M.; Burkholder, J.B.; Fernandez, R.P.; Froidevaux, L.; Hall, B.D.; Hossaini, R.; Saito, T.; Vollmer, M.K.; Yao, B. Chapter 1: Update on Ozone Depleting Substances (ODSs) and Other Gases of Interest to the Montreal Protocol. In *Scientific Assessment of Ozone Depletion: 2018*; World Meteorological Organization: Geneva, Switzerland, 2019.
14. Prinn, R.G.; Weiss, R.F.; Arduini, J.; Arnold, T.; DeWitt, H.L.; Fraser, P.J.; Ganesan, A.L.; Gasore, J.; Harth, C.M.; Hermansen, O.; et al. History of chemically and radiatively important atmospheric gases from the Advanced Global Atmospheric Gases Experiment (AGAGE). *Earth Syst. Sci. Data* **2018**, *10*, 985–1018, doi:10.5194/essd-10-985-2018.
15. Yoshida, Y.; Wang, Y.; Shim, C.; Cunnold, D.; Blake, D.R.; Dutton, G.S. Inverse modeling of the global methyl chloride sources. *J. Geophys. Res*. **2006**, *111*, D16307, doi:10.1029/2005JD006696.
16. Crippa, M.; Janssens-Maenhout, G.; Dentener, F.; Guizzardi, D.; Sindelarova, K.; Muntean, M.; Van Dingenen, R.; Granier, C. Forty years of improvements in European air quality: Regional policy-industry interactions with global impacts. *Atmos. Chem. Phys*. **2016**, *16*, 3825–3841, doi:10.5194/acp-16-3825-2016.
17. ACTRIS-2 Mt Cimone and Po Valley Field Campaign 2017. http://actris-cimone.isac.cnr.it/ (accessed on 28 February 2020).
18. Campbell, J.E.; Whelan, M.E.; Seibt, U.; Smith, S.J.; Berry, J.A.; Hilton, T.W. Atmospheric carbonyl sulfide sources from anthropogenic activity: Implications for carbon cycle constraints. *Geophys. Res. Lett.* **2015**, *42*, 3004–3010, doi:10.1002/2015GL063445.
19. Whelan, M.E.; Lennartz, S.T.; Gimeno, T.E.; Wehr, R.; Wohlfahrt, G.; Wang, Y.; Kooijmans, L.M.J.; Hilton, T.W.; Belviso, S.; Peylin, P.; et al. Reviews and syntheses: Carbonyl sulfide as a multi-scale tracer for carbon and water cycles. *Biogeosciences* **2018**, *15*, 3625–3657, doi:10.5194/bg-15-3625-2018.
20. Cristofanelli, P.; Landi, T.C.; Calzolari, F.; Duchi, R.; Marinoni, A.; Rinaldi, M.; Bonasoni, P. Summer atmospheric composition over the Mediterranean basin: Investigation on transport processes and pollutant export to the free troposphere by observations at the WMO/GAW Mt. Cimone global station (Italy, 2165 m a.s.l.). *Atmos. Environ.* **2016**, *141*, 139–152, doi:10.1016/j.atmosenv.2016.06.048.
21. Cristofanelli, P.; Brattich, E.; Decesari, S.; Landi, T.C.; Maione, M.; Putero, D.; Tositti, L.; Bonasoni, P. *High Mountain Atmospheric Research—The Italian Mt. Cimone WMO/GAW Global Station (2165 m a.s.l.)*; Springer: Amsterdam, The Netherland, 2018; pp. 1–135.
22. Lo Vullo, E.; Furlani, F.; Arduini, J.; Giostra, U.; Graziosi, F.; Cristofanelli, P.; Williams, M.L.; Maione, M. Anthropogenic non-methane volatile hydrocarbons at Mt. Cimone (2165 m a.s.l, Italy): Impact of sources and transport on atmospheric composition. *Atmos. Environ.* **2016**, *140*, 395–403, doi:10.1016/j.atmosenv.2016.05.060.
23. Umezawa, T.; Baker, A.K.; Oram, D.; Sauvage, C.; O'Sullivan, D.; Rauthe-Schöch, A.; Montzka, S.A.; Zahn, A.; Brenninkmeijer, C.A.M. Methyl chloride in the upper troposphere observed by the CARIBIC passenger aircraft observatory: Large-scale distributions and Asian summer monsoon outflow. *J. Geophys. Res. Atmos.* **2014**, *119*, 5542–5558, doi:10.1002/2013JD021396.
24. Simmonds, P.G.; O'Doherty, S.; Derwent, R.G.; Manning, A.J.; Ryall, D.B.; Fraser, P.; Porter, L.; Krummel, P.; Weiss, R.; Miller, B.; et al. AGAGE observations of methyl bromide and methyl chloride at the Mace Head, Ireland and Cape Grim, Tasmania, 1998–2001. *J. Atmos. Chem.* **2004**, *47*, 243–269.

25. Cleveland, W.S.; Grosse, E.; Shyu, W.M. Local regression models. In *Statistical Models in S*; Chambers, J.M., Hastie, T.J., Eds.; Chapman & Hall: New York, NY, USA, 1993; pp. 309–376.
26. Chevalier, A.; Gheusi, F.; Delmas, R.; Ordóñez, C.; Sarrat, C.; Zbinden, R.; Thouret, V.; Athier, G.; Cousin, J.-M. Influence of altitude on ozone levels and variability in the lower troposphere: A ground-based study for western Europe over the period 2001–2004. *Atmos. Chem. Phys*. **2007**, *7*, 4311–4326, doi:10.5194/acp-7-4311-2007.
27. Putero, D.; Cristofanelli, P.; Marinoni, A.; Adhikary, B.; Duchi, R.; Shrestha, S.D.; Verza, G.P.; Landi, T.C.; Calzolari, F.; Busetto, M.; et al. Seasonal variation of ozone and black carbon observed at Paknajol, an urban site in the Kathmandu Valley, Nepal. *Atmos. Chem. Phys*. **2015**, *15*, 13957–13971, doi:10.5194/acp-15-13957-2015.
28. Schultz, M.G.; Akimoto, H.; Bottenheim, J.; Buchmann, B.; Galbally, I.E.; Gilge, S.; Helmig, D.; Koide, H.; Lewis, A.C.; Novelli, P.C.; et al. The Global Atmosphere Watch reactive gases measurement network. *Elem. Sci. Anthr.* **2015**, *3*, 000067, doi:10.12952/journal.elementa.000067.
29. Morgan, W.T.; Allan, J.D.; Bower, K.N.; Highwood, E.J.; Liu, D.; McMeeking, G.R.; Northway, M.J.; Williams, P.I.; Krejci, R.; Coe, H. Airborne measurements of the spatial distribution of aerosol chemical composition across Europe and evolution of the organic fraction. *Atmos. Chem. Phys*. **2010**, *10*, 4065–4083, doi:10.5194/acp-10-4065-2010.
30. Parrish, D.D.; Allen, D.T.; Bates, T.S.; Estes, M.; Fehsenfeld, F.C.; Feingold, G.; Ferrare, R.; Hardesty, R.M.; Meagher, J.F.; Nielsen-Gammon, J.W.; et al. Overview of the Second Texas Air Quality Study (TexAQS II) and the Gulf of Mexico Atmospheric Composition and Climate Study (GoMACCS). *J. Geophys. Res.* **2009**, *114*, D00F13, doi:10.1029/2009JD011842.
31. Carslaw, D.C.; Beevers, S.D. Characterising and understanding emission sources using bivariate polar plots and k-means clustering. *Environ. Model. Soft.* **2013**, *40*, 325–329.
32. Westmoreland, E.J.; Carslaw, N.; Carslaw, D.C.; Gillah, A.; Bates, E. Analysis of air quality within a street canyon using statistical and dispersion modelling techniques. *Atmos. Environ.* **2007**, *41*, 9195–9205.
33. Carslaw, D.C.; Ropkins, K. Openair—An R package for air quality data analysis. *Environ. Model. Soft.* **2012**, *27–28*, 52–61, doi:10.1016/j.envsoft.2012.09.005.
34. Hastie, T.J.; Tibshirani, R. *Generalized Additive Models*; Chapman and Hall: London, UK, 1990; pp. 109.
35. Wood, S.N. *Generalized Additive Models: An Introduction with R*, 3rd ed.; Chapman and Hall/CRC, Taylor & Francis Group: Boca Raton, FL, USA, 2017; pp. 1–457.
36. Marenco, F.; Bonasoni, P.; Calzolari, F.; Ceriani, M.; Chiari, M.; Cristofanelli, P.; D'Alessandro, A.; Fermo, P.; Lucarelli, F.; Mazzei, F.; et al. Characterization of atmospheric aerosols at Monte Cimone, Italy, during summer 2004: Source apportionment and transport mechanisms. *J. Geophys. Res.* **2006**, *111*, D24202, doi:10.1029/2006JD007145.